

Injectable and macroporous calcium phosphate cement scaffold

Hockin H.K. Xu*, Michael D. Weir, Elena F. Burguera¹, Alexis M. Fraser²

Paffenbarger Research Center, 100 Bureau Drive, Stop 8546, American Dental Association Foundation, National Institute of Standards and Technology, Gaithersburg, MD 20899-8546, USA

Received 25 August 2005; accepted 1 March 2006
Available online 2 May 2006

Abstract

Calcium phosphate cement (CPC) can be molded and self-hardens *in vivo* to form resorbable hydroxyapatite with excellent osteoconductivity. The objective of this study was to develop an injectable, macroporous and strong CPC, and to investigate the effects of porogen and absorbable fibers. Water-soluble mannitol was used as porogen and mixed with CPC at mass fractions from 0% to 50%. CPC with 0–40% mannitol was fully extruded under a syringe force of 10 N. The paste with 50% mannitol required a 100-N force which extruded only 66% of the paste. At fiber volume fraction of 0–5%, the paste was completely extruded. However, at 6% and 7.5% fibers, some fibers were left in the syringe after the paste was extruded. The injectable CPC scaffold had a flexural strength (mean \pm sd; $n = 5$) of (3.2 ± 1.0) MPa, which approached the reported strengths for sintered porous hydroxyapatite implants and cancellous bone. In summary, the injectability of a ceramic scaffold, a macroporous CPC, was studied for the first time. Processing parameters were tailored to achieve high injectability, macroporosity, and strength. The injectable and strong CPC scaffold may be useful in surgical sites that are not freely accessible by open surgery or when using minimally invasive techniques.

© 2006 Elsevier Ltd. All rights reserved.

Keywords: Calcium phosphate cement; Injectability; Macroporous scaffold; Strength; Bone repair

1. Introduction

The need for biomaterials has increased as the world population ages, and calcium phosphate ceramics have gained clinical acceptance for bone substitution and augmentation [1–5]. This is because calcium phosphates consist of the same ions as the mineral in natural bones. Hydroxyapatite ceramic implants have produced no toxicity, no inflammation, and no foreign body response *in vivo*. New bone has been observed to grow on the hydroxyapatite implant surfaces without an intervening fibrous layer, and fracture tests have shown cracking through the bone or the hydroxyapatite implant, but not the bone-implant interface [4,6]. In addition, porous calcium phosphate scaffolds have been developed to facilitate cell infiltration and tissue ingrowth [7–11].

A major disadvantage of current orthopaedic implants is that they exist in hardened forms, requiring the surgeon to fit the surgical site around the implant or to carve the graft to the desired shape. This can lead to increases in bone loss, trauma to the surrounding tissue, and prolonged surgical time [12]. In contrast, calcium phosphate cements (CPCs) can self-set in the bone cavity without machining. The first CPC was developed in 1986 [13]. Since then, many compositions have been reported [14–21]. The CPC powder can be mixed with an aqueous liquid to form a paste that can be placed in the bone cavity to form hydroxyapatite [17]. Due to its excellent osteoconductivity and bone replacement capability, CPC is highly promising for clinical applications [13,17,22,23]. However, the drawbacks of CPC, including the lack of macroporosity for bone ingrowth, low strength [22,23], and poor injectability [24], have limited its clinical use.

The injectability of CPC is important in clinical applications that involve defects with limited accessibility or narrow cavities, when there is a need for precise placement of the paste to conform to a defect area, or when using minimally invasive surgical techniques [25–30].

*Corresponding author. Tel.: +301 975 6804; fax: +301 963 9143.

E-mail address: hockin.xu@nist.gov (H.H.K. Xu).

¹Now with Materials Science and Engineering Department, Virginia Polytechnic Institute and State University, Blacksburg, VA.

²Colgate-Palmolive Student Scholar Intern, Cornell University, Ithaca, NY.

A recent study investigated the injectability of a CPC consisting of dicalcium phosphate dihydrate and tetracalcium phosphate [31]. The incorporation of a gelling agent (hydroxypropyl methylcellulose) dramatically improved the injectability of the CPC paste [31]. However, in the previous study, the injectable CPC had no macropores for cell infiltration and tissue ingrowth. Furthermore, the injectable CPC contained no fibers that could provide strength and fracture resistance for stress-bearing applications [32,33]. A literature search revealed no previous report on developing an injectable and macroporous ceramic scaffold.

Accordingly, the objective of the present study was to develop an injectable, macroporous and strong CPC scaffold, and to investigate the effects of porogen and fiber contents on the injectability and mechanical properties. The hypotheses to be tested were: (1) CPC could be rendered injectable even when the paste contains macropore-forming particles (porogens) and reinforcing fibers; and (2) the porogen content and fiber volume fraction would significantly affect the injectability, scaffold porosity, and mechanical properties.

2. Materials and methods

2.1. Cement powder and liquid

The processing of the CPC powder was described previously [13,33]. Briefly, tetracalcium phosphate (TTCP: $\text{Ca}_4(\text{PO}_4)_2\text{O}$) was synthesized from a solid-state reaction between CaHPO_4 and CaCO_3 (J.T. Baker Chemical, Phillipsburg, NJ), which were mixed and heated at 1500°C for 6 h in a furnace (Model 51333, Lindberg, Watertown, WI). The mixture was ground and sieved to obtain TTCP particles with sizes ranging from about 1 to $60\ \mu\text{m}$, with an average size of $20\ \mu\text{m}$.

When commercial dicalcium phosphate dihydrate (DCPD, $\text{CaHPO}_4 \cdot 2\text{H}_2\text{O}$) powders were used, the resulting TTCP-DCPD pastes exhibited undesirably long setting times, likely due to impurities in the commercial powders [34]. Hence DCPD was synthesized in our laboratory. The pH of a DCPD-monocalcium phosphate monohydrate singular point solution (pH = 1.9, 4°C) was slowly raised via the addition of CaCO_3 . The DCPD that precipitated before pH reaching 3.5 (below the hydroxyapatite-DCPD singular point of 4.2) was collected to avoid possible contamination by hydroxyapatite. The DCPD was thoroughly washed, first with distilled water, and then with ethanol, to eliminate residual acid components. The washed DCPD was dried at room temperature in the hood with a constant flow of dry air for 3 days. This was because DCPD could convert to DCPA if a high temperature was used in the drying process or if significant moisture was present. The DCPD powder thus dried was stored in closed containers in a refrigerator for one year in preliminary studies, and no conversion to DCPA was detected with a powder X-ray diffractometer (Rigaku, Danvers, MA). The DCPD powder was ground to obtain particles with sizes ranging from 0.5 to $4\ \mu\text{m}$, with an average size of $1.3\ \mu\text{m}$. The ground DCPD powder was mixed with the TTCP powder at a molar ratio of 1:1 to form the CPC powder.

Water-soluble mannitol was used as a porogen because it has the appropriate solubility and is non-toxic [33,35]. Mannitol ($\text{CH}_2\text{OH}[\text{CHOH}]_4\text{CH}_2\text{OH}$, Sigma, St. Louis, MO) was recrystallized in an ethanol/water solution at 50/50 by volume, dried, ground, and sieved through openings of $500\ \mu\text{m}$ (top sieve) and $300\ \mu\text{m}$ (bottom sieve). The mannitol particles were mixed with the CPC powder at mannitol/(mannitol+CPC powder) mass percentages of: 0%, 20%, 30%, 40%, and 50%.

The cement liquid contained sodium phosphate as a hardening accelerator and hydroxypropyl methylcellulose (HPMC) as a gelling agent [36,37]. A commercial sodium phosphate solution (3 mol/L Na_2HPO_4 and NaH_2PO_4 , Abbott, North Chicago, IL) was diluted with distilled water to obtain a sodium phosphate concentration of 0.2 mol/L [31]. Then, HPMC (Sigma, St. Louis, MO) was added to the solution at a HPMC mass fraction of 1%. This mass fraction was selected because it improved the cohesiveness and injectability of the CPC paste [31].

2.2. Setting time

The powder and liquid were mixed with a spatula at a CPC powder:liquid mass ratio of 2:1 following a previous study [31]. The paste was filled into a mold of 6 mm diameter and 3 mm depth and incubated in a humidior with 100% relative humidity at 37°C [36–38]. Following the method used in previous studies, when the powder component of the specimen did not come off when scrubbed gently with fingers, the setting reaction had occurred enough to hold the specimen together [36–38]. The time measured from the start of powder-liquid mixing to this point was used as the setting time [36–38].

2.3. Density and porosity

Specimens were allowed to set in molds of 6 mm diameter and 3 mm depth for 4 h, then demolded and immersed in distilled water for 20 h at 37°C . The immersion dissolved the mannitol and created macropores in the set CPC [33]. The specimens were then dried in a vacuum oven (American Scientific Products, McGaw Park, IL) at 60°C for 24 h. The specimen density was measured as mass/volume [33]. A previous study showed that this method yielded density values that closely matched those measured by a mercury intrusion porosimetry method [33].

The measured specimen density d_{measured} yields the total porosity P_{total} :

$$P_{\text{total}} = (d_{\text{HA}} - d_{\text{measured}})/d_{\text{HA}}, \quad (1)$$

where d_{HA} is the density of fully dense hydroxyapatite which is $3.14\ \text{g}/\text{cm}^3$ [35]. The total porosity has two parts: the intrinsic microporosity of the CPC without mannitol, and the macroporosity from the dissolution of mannitol particles, P_{mannitol} . As described in previous studies [33,37], P_{mannitol} can be calculated by

$$P_{\text{mannitol}} = 1 - d_{\text{measured}}/d_{\text{measured-0\%}}, \quad (2)$$

where $d_{\text{measured-0\%}}$ is the density of CPC with 0% mannitol.

2.4. Injectability

A 10 mL syringe (Free-Flo, Kerr, Romulus, MI) with a diameter of 10 mm, similar to those in previous studies [25,26], was used. The orifice inner diameter was 2.8 mm, similar to a commercial 10-gauge needle having a 2.7 mm inner diameter. The CPC powder:liquid ratio was 2:1, with 2 g of powder and 1 g of liquid [31]. The paste was mixed using an automatic mixer (Maxi Mix, Thermolyne, Dubuque, IA) for 15 s [31] and then placed into the syringe. The syringe was placed between the compression plates of a computer-controlled Universal Testing Machine (5500R, MTS, Cary, NC). At a prescribed time from the start of mixing, compression was started on the syringe plunger. The cement was extruded at a crosshead speed of 15 mm/min until a maximum force of 100 N was achieved, following the method of previous studies [25,26]. Two parameters were measured. First, the injection force was recorded by the computer. Second, the percentage of extruded paste was determined as the mass of the paste that could be extruded from the syringe divided by the original mass of the paste inside the syringe [25,26,29].

Three groups of specimens were tested for injectability. The first group was to study the effect of mannitol content on injectability. This group consisted of the CPC-mannitol composites with mannitol mass percentages of 0%, 20%, 30%, 40%, and 50%. The time from the start of the cement powder-liquid mixing to the start of extruding the paste was 1.5 min [25,26].

The second group was to vary the time from the start of mixing to the start of injection, referred to as “time after start of mixing”. The purpose was to examine how much working time the surgeon would have before the injectability of the paste was compromised due to setting in the syringe. An intermediate mannitol percentage of 30% was used for this group. Four times after the start of mixing were tested: 1.5, 5, 10, and 15 min. They were selected because 15 min would provide the clinician with ample working time from mixing the paste to applying the paste.

The third group was to study the effect of fiber content in CPC-mannitol-fiber pastes on injectability. The mannitol mass percentage was fixed at 30%, and the time after the start of mixing was 1.5 min. An absorbable suture fiber (Vicryl, Ethicon, Somerville, NJ) was selected because it is clinically used as a suture material and possesses a relatively high strength [39]. The suture consisted of individual fibers braided into a bundle with a diameter of 322 μm . The suture was cut to filaments of 5 mm in length. The filaments were added to the CPC powder and liquid which were mixed on the mixer for 15 s as described above. The 5 mm length was selected because the fibers of 3 mm length did not significantly increase the CPC strength, while the fibers of 8 mm length rendered the paste difficult to be injected. The fiber volume fraction (fiber volume/total specimen volume) was varied from 0%, 2.5%, 5.0%, 6.0%, to 7.5%. Fractions higher than 7.5% were not tested because the composite paste became too difficult to extrude.

2.5. Mechanical properties

Molds of 3 mm \times 4 mm \times 25 mm were used to make specimens [33]. Each specimen was allowed to set in the humidior at 37°C for 4 h, then demolded and immersed in distilled water at 37°C for 20 h. The mannitol mass percentage was 30%. The fiber volume percentage was varied from 0%, 2.5%, 5.0%, to 6.0%. Fiber volume percentage of 7.5% was not tested because the injection test above showed that some fibers remained in the syringe when the paste was extruded. Specimens were fractured using a three-point flexural test with a 20 mm span at a crosshead speed of 1 mm/min on the Universal Testing Machine. As described previously [40,41], flexural strength, elastic modulus and work-of-fracture (toughness) were determined.

Selected specimens were sputter coated with gold and examined using a scanning electron microscope (SEM, JEOL 5300, Peabody, MA). One-way ANOVA was performed to detect the significant effects. Tukey's multiple comparison test was used at $p = 0.05$.

3. Results

3.1. Effects of mannitol content on setting time

Cement setting time vs. mannitol mass fraction is listed in Table 1. Setting time was significantly increased from 0% mannitol to 20% mannitol ($p < 0.001$). There was no further significant increase in setting time when the mannitol mass fraction was increased from 20% to 50% (Tukey's multiple comparison test at $p = 0.05$).

3.2. Effects of mannitol content on density and porosity

The density and porosity values are listed in Table 2. The specimens were immersed for 1 d which dissolved the mannitol particles and created macropores in CPC. One-way ANOVA identified a significant effect ($p < 0.001$) of mannitol content on the specimen density ($p < 0.001$). The corresponding total porosity and macroporosity were obtained from Eqs. (1) and (2).

Table 1

Cement setting time^a vs. mass fraction of mannitol porogen to form macropores

Mannitol mass fraction (%)	Cement setting time (min)
0	11.0 \pm 1.2
20	15.3 \pm 1.2
30	15.0 \pm 0.8
40	15.0 \pm 0.8
50	15.5 \pm 1.0

^aValues are mean \pm sd; $n = 4$. Setting time was measured as described in Section 2.2.

Table 2

Density^a, total porosity and macroporosity of CPC scaffold vs. mannitol mass fraction

Mannitol mass fraction (%)	Density (g/cm ³)	Total pore volume fraction (%)	Macropore volume fraction (%)
0	1.11 \pm 0.04	64.6 \pm 1.3	0
20	0.90 \pm 0.05	71.4 \pm 1.6	19.4 \pm 4.6
30	0.72 \pm 0.05	77.2 \pm 1.7	35.7 \pm 4.9
40	0.55 \pm 0.08	82.6 \pm 2.4	50.9 \pm 6.7
50	0.56 \pm 0.02	82.0 \pm 0.7	49.3 \pm 1.9

^aThe CPC scaffold density (mean \pm sd; $n = 5$) was measured as described in Section 2.3. Total porosity and macroporosity were calculated using Eqs. (1) and (2), respectively.

3.3. Effects of mannitol content on injectability

Fig. 1 shows examples of injection force vs. syringe plunger displacement. A typical curve for an injectable paste is shown in (A) for a CPC paste containing 30% mannitol. In contrast, the paste in (B) containing 50% mannitol was relatively difficult to extrude. The paste in (A) was completely extruded at an injection force of about 8 N, while only 66% of the paste was extruded in (B) when the injection force reached 100 N. The test was stopped at 100 N because higher forces may not be practical in manual injection during surgery [25,26]. The long arrow in (A) indicates the high force region caused by the plunger touching the end of the syringe when all the paste was extruded. The short arrow in (A) indicates the highest injection force for this paste which was used as the maximum injection force in Fig. 2.

The maximum injection force vs. mannitol mass fraction is plotted in Fig. 2. The paste containing 50% mannitol had a percentage of extruded paste (mean \pm sd; $n = 4$) of (66 \pm 30) % when the injection force reached 100 N. The other pastes with mannitol mass fractions ranging from 0% to 40% were completely extruded out of the syringe under forces of 10 N or less, and the injection forces were not significantly different from each other (Tukey's at $p = 0.05$).

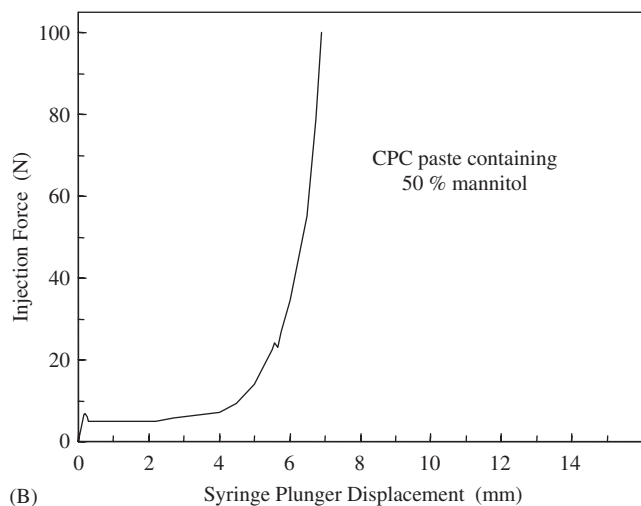
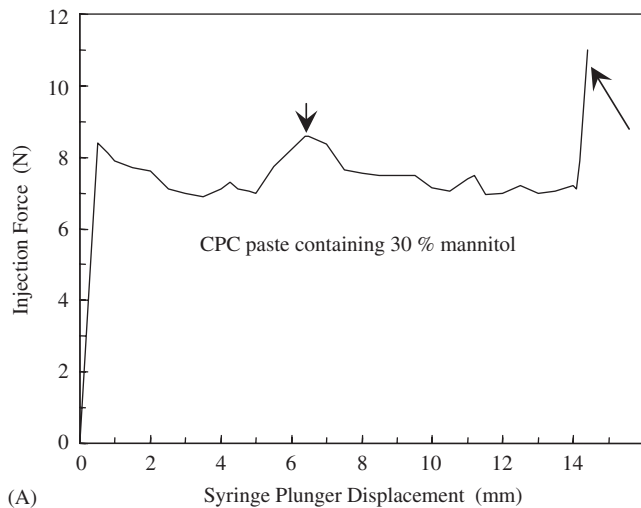


Fig. 1. Injection force vs. syringe plunger displacement for CPC paste with (A) 30% mannitol, and (B) 50% mannitol. The paste in (A) was fully extruded under a force of 8 N. The paste in (B) was difficult to extrude, with 66% of the paste extruded at 100 N. The test was stopped at 100 N to be feasible for manual injection clinically. The long arrow in (A) indicates where the plunger was touching the end of the syringe when all the paste was extruded (the mass percentage of extruded paste was measured to be 98%). The short arrow in (A) indicates the maximum injection force.

3.4. Effects of time after start of mixing on injectability

Fig. 3 plots the maximum injection force vs. the time after the start of paste mixing. The mannitol mass fraction was fixed at 30%. The pastes at 1.5–15 min were all completely extruded out of the syringe. However, one-way ANOVA showed a significant increase in the injection force with time after the start of mixing ($p < 0.05$). The injection forces (mean \pm sd; $n = 4$) at 1.5–10 min, though increasing, were not significantly different from each other; the force at 15 min reached (48.9 ± 12.2) N, which was significantly higher than the others ($p < 0.05$).

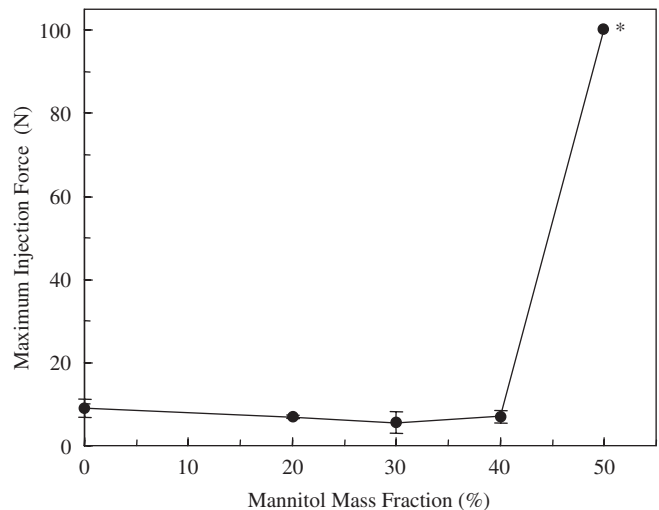


Fig. 2. Maximum injection force vs. mannitol percentage in CPC. The time after the start of paste mixing to injection was 1.5 min. All the pastes were completely extruded out of the syringe for 0–40% mannitol (the mass percentage of extruded paste was measured to be 98%). The paste containing 50% mannitol had a percentage of extruded paste (mean \pm sd; $n = 4$) of (66 ± 30)%. The * indicates that the test was stopped at 100 N. Each value was mean \pm sd; $n = 4$. The line connects the data points for visual clarity.

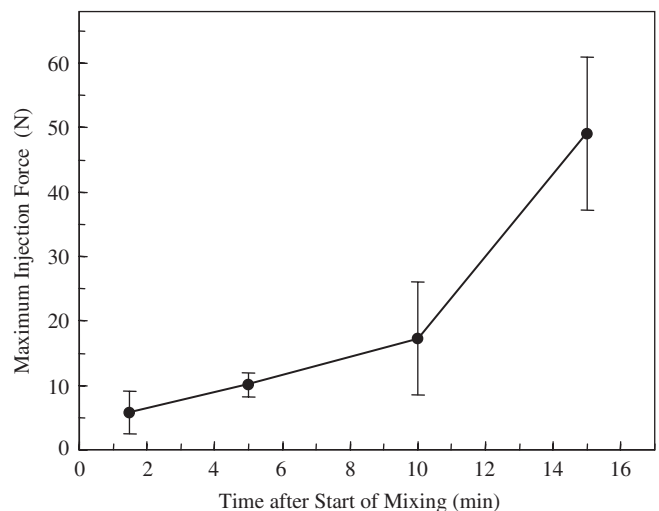


Fig. 3. Maximum injection force vs. the time after the start of CPC paste mixing. The mannitol percentage was 30%. All the pastes from 1.5 to 15 min were completely extruded (the percentage of extruded paste was measured to be 98%). The corresponding injection force monotonically increased with increasing the time after the start of paste mixing. Each value was mean \pm sd; $n = 4$. The line connects the data points for visual clarity.

3.5. SEM examination

SEM micrographs of CPC scaffolds are shown in Fig. 4 for (A) 0% mannitol, (B) 30% mannitol, (C) 40% mannitol, and (D) 40% mannitol at a higher magnification. CPC without mannitol had only micropores without

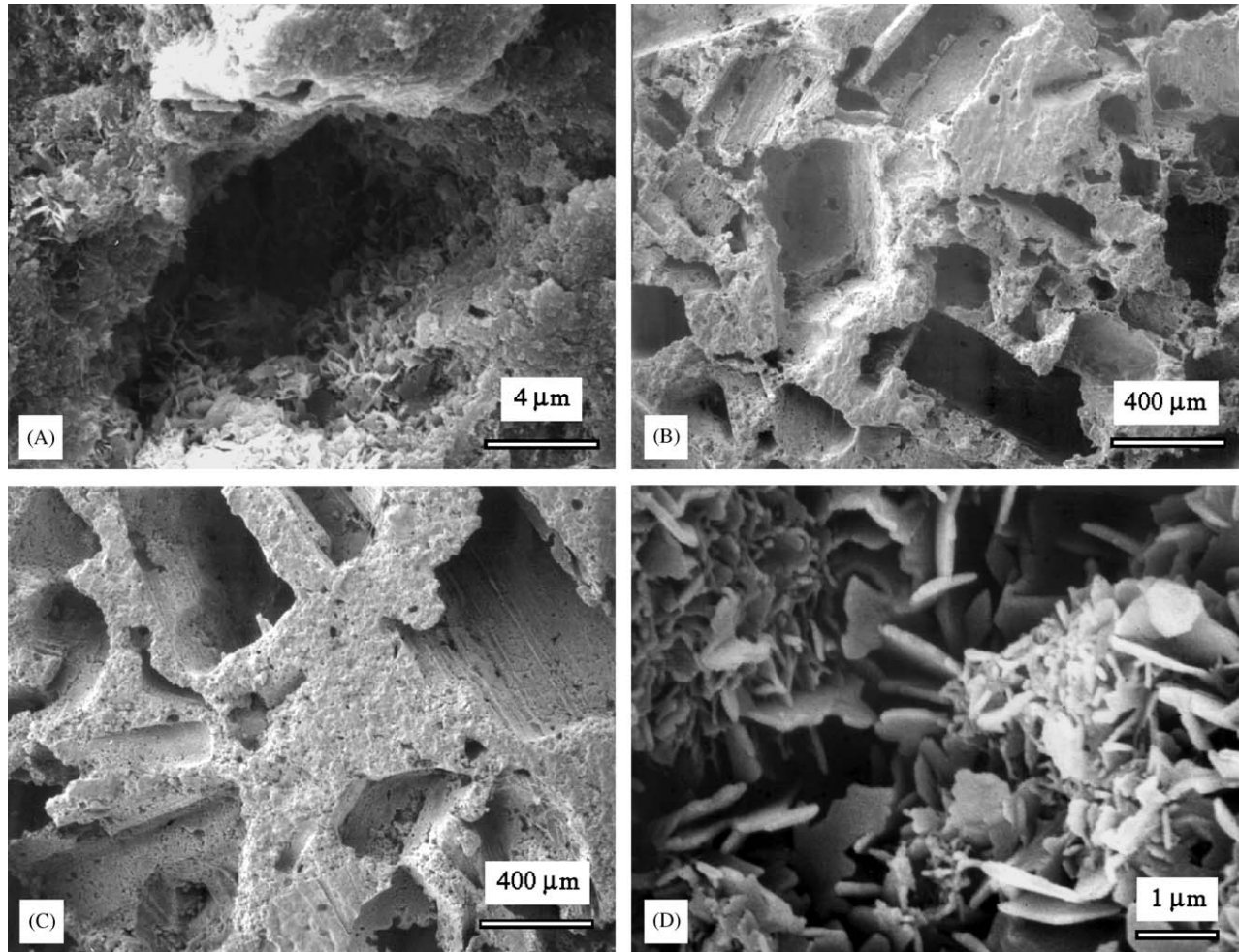


Fig. 4. SEM micrographs of CPC scaffolds for (A) 0% mannitol, (B) 30% mannitol, (C) 40% mannitol, and (D) 40% mannitol at a higher magnification. Note that (A) had a higher magnification in order to reveal the details of a micropore. The micropores had sizes ranged from about 1 to 20 μm . The macropores in (B) and (C) were produced by the dissolution of the mannitol porogen, with a width of about 100–400 μm , and a length of 200–600 μm . Nano-sized hydroxyapatite crystallites that make up the cement specimens are shown in (D).

macropores. The micropore size ranged from about 1 to 20 μm . The macropores in (B) and (C) were well-formed in the shapes of the entrapped mannitol crystals. They were slightly elongated, having a width of about 100–400 μm , and a length of 200–600 μm . Examination of various specimens revealed no noticeable differences in pore size or shape at different mannitol mass fractions. Examples of the hydroxyapatite crystallites that make up the specimen are shown in (D). The crystals were generally in the nanosize range, with a short dimension of about 100 nm and a long dimension of 300 nm to 1 μm . The larger crystals appeared to be platelets, with a thickness of about 200 nm and a width of 500 nm to 2 μm . Similar crystals were observed in specimens with different mannitol fractions.

3.6. Effects of fiber volume fraction on injectability

Fig. 5 plots injection force vs. fiber volume fraction. The mannitol mass fraction was fixed at 30%, and the time after the start of paste mixing was 1.5 min. The injection forces, varying from about 6 to 10 N, were in general not

very different from each other. At 6% and 7.5% fibers (indicated by the * in Fig. 5), some fibers were left behind in the syringe while the paste was extruded. In contrast, at fiber volume percentages from 0% to 5%, the composite paste was fully extruded. At 6% and 7.5% fibers, the percentages of extruded paste (mean \pm sd; $n = 4$) became $(94 \pm 6) \%$ and $(89 \pm 8) \%$, respectively.

3.7. Mechanical properties of injectable CPC scaffold

Mechanical properties vs. fiber volume fraction are plotted in Fig. 6. The mannitol was 30% and the specimens were immersed for 1 d to dissolve the mannitol and create macropores. One-way ANOVA revealed a significant effect of fiber volume fraction on strength and work-of-fracture ($p < 0.001$), but not on elastic modulus ($p = 0.286$). The flexural strength (mean \pm sd; $n = 5$) was (3.2 ± 1.0) MPa for specimens containing 5% fibers. It was significantly higher ($p < 0.05$) than (1.0 ± 0.2) MPa for the specimens with 2.5% fibers and (1.1 ± 0.3) MPa for the specimens with 0% fibers ($p < 0.05$).

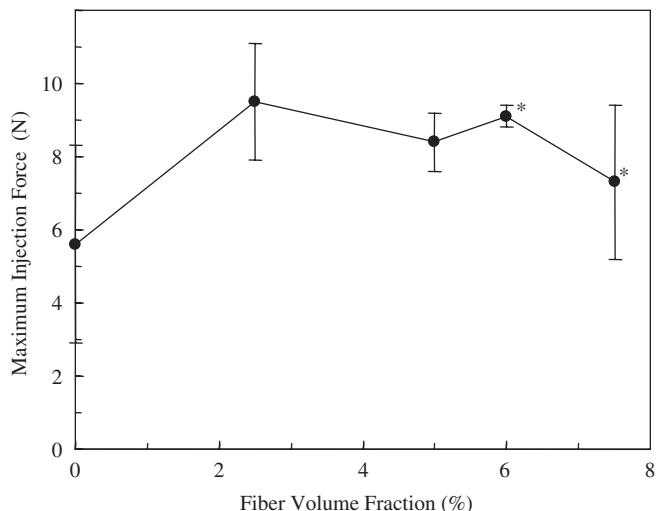


Fig. 5. Injection force vs. fiber volume fraction for CPC-mannitol-absorbable fiber pastes. The mannitol percentage was 30%, and the time after start of paste mixing was 1.5 min. At 6% and 7.5% fibers (*), some fibers remained in the syringe while the paste was extruded. At 0% to 5% fibers, the mass percentage of extruded paste was 98%. At 6% and 7.5% fibers, the percent of extruded paste was (94 ± 6) % and (89 ± 8) %, respectively. Each value was mean \pm sd; $n = 4$. The line connects the data points for visual clarity.

The work-of-fracture was (331 ± 78) J/m² for the specimens with 5% fibers, a 36-fold increase over the (9.1 ± 2.6) J/m² for the specimens with 0% fibers. Elastic modulus insignificantly varied between 1 and 1.5 GPa, as the soft fibers did not increase the modulus of the specimens.

4. Discussion

In the present study, an injectable and macroporous CPC scaffold was developed using DCPD, a hardening accelerator, a gelling agent and a porogen. Hydroxyapatite and other calcium phosphate-based ceramic scaffolds were developed as pre-formed implants in previous studies [4,7–11]. Based on our literature search, this represents the first study on the injectability of an injectable ceramic scaffold. Improving the injectability of the CPC paste can inadvertently prolong the cement setting time. For example, the addition of glycerol improved the injectability of a CPC, but greatly increased the time it took for the cement to harden [42]. A long setting time could cause problems because of the cement's inability to support stresses within this time period [16]. For example, a severe inflammatory response occurred when the CPC failed to set and disintegrated, likely due to a low initial mechanical strength [16,43]. The dilemma is that a paste capable of setting rapidly may start setting in the syringe, thereby increasing the paste rigidity and reducing its injectability. The components used in the injectable CPC of the present study enabled the cement to be fully injectable while at the same time providing a rapid setting ability (Table 1).

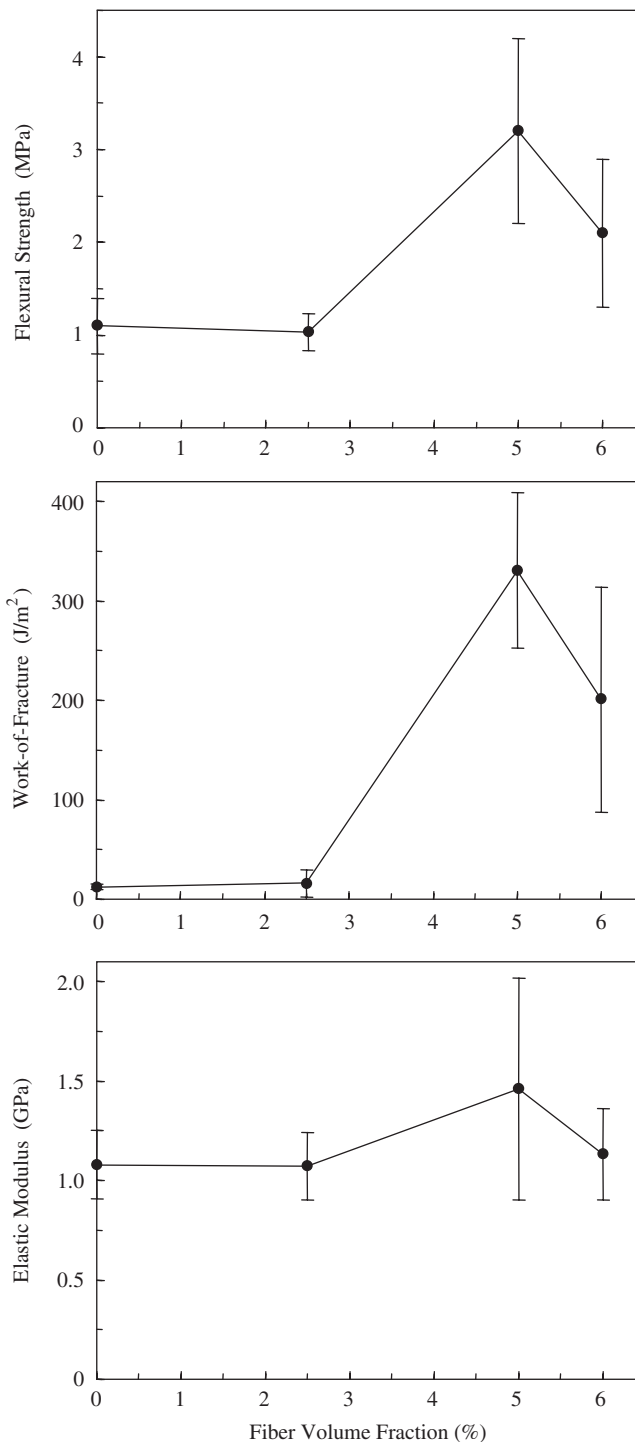


Fig. 6. Mechanical properties vs. fiber volume fraction for CPC-mannitol-absorbable fiber composite. The mannitol mass fraction was 30% and the specimens were immersed for 1 d to dissolve the mannitol and create macropores. Each value was mean \pm sd; $n = 5$. The lines connect the data points for visual clarity.

This was achieved because DCPD and the hardening accelerator imparted fast-setting to the cement, while HPMC simultaneously improved the paste cohesiveness and injectability. A previous study showed that the CPC consisting of TTCP-DCPD had a setting time of 15 min,

while that consisting of TTCP-DCPA (dicalcium phosphate anhydrous) was 80 min [44]. TTCP and DCPD dissolve in water as Ca^{2+} , PO_4^{3-} and OH^- ions, which then reprecipitate to form hydroxyapatite: $2\text{Ca}_4(\text{PO}_4)_2\text{O} + 2\text{CaHPO}_4 \cdot 2\text{H}_2\text{O} \rightarrow \text{Ca}_{10}(\text{PO}_4)_6(\text{OH})_2 + 4\text{H}_2\text{O}$. Therefore, DCPD, known to have a relatively high solubility [13], accelerated the setting reaction [44]. Furthermore, the hardening accelerator, sodium phosphate, increased the phosphate concentration and hence accelerated the setting reaction. DCPD and sodium phosphate together helped achieve a fast setting time of about 15 min even with the addition of the mannitol porogen (Table 1). This is consistent with a previous study showing that the conversion to hydroxyapatite for TTCP-DCPD was higher in the first 2 h after paste-mixing, but lower at 24 h, compared to the TTCP-DCPA cement [31].

Another important component in the cement was the gelling agent. HPMC is a derivative of cellulose which is one of the most common polysaccharides [36–38]. HPMC can hydrogen bond to water and form a viscous solution, thus improving the paste's cohesiveness [36–38]. It was observed that when a powder and a liquid were mixed into a paste and delivered through a cannula, a filter-pressing phenomenon occurred in which the liquid was pushed out but a major portion of the powder remained inside the syringe, leading to a phase separation of the liquid and the solid [29]. The presence of HPMC may make it more difficult for the solid–liquid phases to separate, thereby enabling the paste to be completely extruded at a relatively small injection force, even with mannitol porogen of up to 40% (Fig. 2). In addition, HPMC may have also had a lubricating effect on the inter-particle contacts in the paste. This is consistent with a previous study that observed an improvement in the paste injectability with the addition of small amounts of a polysaccharide xanthan, likely a result of a lubricating effect [30].

At 10 min after the start of paste mixing, which should provide sufficient working time clinically, the force under which the paste was fully injected was relatively low at 16.3 N (Fig. 3). However, the injection force was increased dramatically at 15 min after the start of paste mixing. This was because this time approached the cement setting time of 15 min (Table 1), at which point the rigidity of the paste increased. Complete setting of the cement usually took 1 d [13]. Hence the cement at 15 min was still injectable at a higher injection force (Fig. 3). Nonetheless, the paste should preferably be injected within about 10 min after the start of mixing, so that the initial setting reaction of the cement would not be disrupted by the injection process. It should also be noted that the exact value of the injection force may change when different types and sizes of syringes are used.

The potential advantages of the injectable CPC include: easy placement in surgery, able to be used in difficult surgical sites that are not freely accessible by open surgery, and capable of filling narrow defects and facilitating minimally invasive techniques. Traditional CPCs exhibited

poor injectability [24,30]. Hence several previous studies were performed to improve the injectability of CPCs, including investigations on the effects of powder-to-liquid ratio [25], particle shape [24] and particle size [30]. The incorporation of a polymeric drug [26] and citric acid [27], and the use of oscillatory mixing [45] and ion modification [29] were also shown to influence the injectability.

Compared to the previous studies, the uniqueness of the present study was that the CPC paste that was extruded from the syringe contained macropore-forming particles and fibers for the first time. Regarding the porosity, sintered hydroxyapatite implants had pore volume fractions of 40% [8], 48% [46], and 75% [9]. They compare with the total porosity for the injectable CPC of 77% and 83%, at 30% and 40% mannitol, respectively. The mannitol mass fraction of 50% did not increase the CPC porosity over that at 40% mannitol (Table 2). After the mannitol was dissolved, the specimens were dried for density measurement. It is possible that the specimen with 50% mannitol may have shrunk slightly during the drying process, thereby compromising the porosity increase. Besides using solid porogen particles such as mannitol, previous studies have also used a foaming agent (a hydrogen peroxide solution) [47] and a hydrophobic liquid (oil) [48] as porogens to fabricate macroporous scaffolds.

Regarding pore size, previous studies showed that pore sizes of at least $100 \mu\text{m}$ were needed for bone ingrowth [46]. Therefore, the micropores in CPC (Fig. 4A) were too small for bone ingrowth. Other studies used hydroxyapatite with pore diameters of $150 \mu\text{m}$ [9] and $100 \mu\text{m}$ [8]. One study [49] tested a series of pore sizes: 106–212, 212–300, 300–400, 400–500, and 500–600 μm . The highest amount of new bone formation was achieved in the implant with 300–400 μm pores [49]. The macropores in Figs. 4B and C appeared to be suitable for cell infiltration and bone ingrowth. In addition, because CPC is bioresorbable [17,22,23], its pore size and porosity are expected to increase with time in vivo.

CPC maintained its injectability at a fiber volume fraction of 5%, requiring an injection force of 8.4 N to fully extrude the paste. For the set scaffold with 5% fibers immersed for 1 d to dissolve the mannitol, the flexural strength reached 3.2 MPa. This approached the reported flexural strength of 2–11 MPa for sintered porous hydroxyapatite implants [4] and a tensile strength of 3.5 MPa for cancellous bone [50]. Cancellous bone had an elastic modulus of about 0.30 GPa [51], compared to about 1 GPa for the injectable CPC scaffold (Fig. 6). In a previous in vitro study, the absorbable fibers provided reinforcement for several weeks, then dissolved and created long cylindrical macropores suitable for cell infiltration [39]. When the fibers gradually dissolved, the mechanical properties of the composite gradually decreased [39]. However, the rationale for using these absorbable fibers was that after several weeks of bone ingrowth into the macropores from the dissolution of mannitol, the scaffold would have been strengthened by the new bone.

For example, it was observed that the flexural strength of hydroxyapatite implants was increased to about 40 MPa after new bone grew into the macropores [5]. Hence the strengthening of the scaffold from bone ingrowth should offset the weakening of the scaffold due to fiber degradation. Animal studies are needed to examine new bone growth into the injectable and macroporous CPC scaffold, and to explore the potential usefulness of the injectable scaffold in various orthopedic applications.

5. Summary

A novel injectable and macroporous CPC was developed via the use of dicalcium phosphate dihydrate, a hardening accelerator, a gelling agent, porogen particles, and absorbable fibers. The injection force, percentage of paste extruded, mechanical properties and porosity were tailored by compositional variables. The injectable scaffolds with 30% and 40% mannitol possessed total porosity values of 77% and 83% (macroporosity of 36% and 51%), respectively. The macropore sizes ranged from 200 to 600 μm . With 5% absorbable fibers, the CPC composite paste was fully extruded under an injection force of 8.4 N. The flexural strength of the scaffold was 3.2 MPa, which approached the reported strengths for sintered porous hydroxyapatite implants and cancellous bone. SEM revealed the formation of nano-sized hydroxyapatite crystals in the scaffold. Literature search suggests that this is the first study on the injectability of a macroporous ceramic scaffold. Potential advantages for the injectable CPC scaffold include: easy placement in surgery; ability to self-harden in situ to form a resorbable macroporous hydroxyapatite; ability to be used in difficult surgical sites that are not freely accessible by open surgery; and being capable of filling narrow defects and facilitating minimally invasive techniques. Further studies are needed to investigate the performance of this injectable scaffold in animal models.

Acknowledgments

We thank Drs. S. Takagi and L.C. Chow for discussions. E.F. Burguera acknowledges the Great-West Life Annuity for support through a scientist-in-training program. A.M. Fraser thanks Colgate-Palmolive for support through a Student Scholars program. This study was supported by USPHS NIH grant R01 DE14190 (to Xu), NIST, and the ADAF.

Disclaimer: Certain commercial materials and equipment are identified in this paper to specify experimental procedures. In no instance does such identification imply recommendation by NIST or the ADA Foundation or that the material identified is necessarily the best available for the purpose. One standard deviation was used as the estimated standard uncertainty of the measurements. These

values should not be compared with data obtained in other laboratories under different conditions.

References

- [1] LeGeros RZ. Biodegradation and bioresorption of calcium phosphate ceramics. *Clin Mater* 1993;14:65–88.
- [2] Thomson RC, Yaszemski MJ, Powers JM, Mikos AG. Hydroxyapatite fiber reinforced poly(α -hydroxy ester) foams for bone regeneration. *Biomaterials* 1998;19:1935–43.
- [3] Hench LL. Biomaterials: A forecast for the future. *Biomaterials* 1998;19:1419–23.
- [4] Suchanek W, Yoshimura M. Processing and properties of hydroxyapatite-based biomaterials for use as hard tissue replacement implants. *J Mater Res* 1998;13:94–117.
- [5] Ducheyne P, Qiu Q. Bioactive ceramics: the effect of surface reactivity on bone formation and bone cell function. *Biomaterials* 1999;20:2287–303.
- [6] Jarcho M. Calcium phosphate ceramics as hard tissue prosthetics. *Clin Orthop* 1981;157:259–78.
- [7] Hing KA, Best SM, Bonfield W. Characterization of porous hydroxyapatite. *J Mater Sci: Mater in Med* 1999;10:135–45.
- [8] Pilliar RM, Filiaggi MJ, Wells JD, Grynblas MD, Kandel RA. Porous calcium polyphosphate scaffolds for bone substitute applications—in vitro characterization. *Biomaterials* 2001;22:963–72.
- [9] Tamai N, Myoui A, Tomita T, Nakase T, Tanaka J, Ochi T, et al. Novel hydroxyapatite ceramics with an interconnective porous structure exhibit superior osteoconduction in vivo. *J Biomed Mater Res* 2002;59:110–7.
- [10] Chu TMG, Orton DG, Hollister SJ, Feinberg SE, Halloran JW. Mechanical and in vivo performance of hydroxyapatite implants with controlled architectures. *Biomaterials* 2002;23:1283–93.
- [11] Grynblas MD, Pilliar RM, Kandel RA, Renlund R, Filiaggi M, Dumitriu M. Porous calcium polyphosphate scaffolds for bone substitute applications in vivo studies. *Biomaterials* 2002;23:2063–70.
- [12] Laurencin CT, Ambrosio AMA, Borden MD, Cooper Jr. JA. Tissue engineering: Orthopedic applications. *Annu Rev Biomed Eng* 1999;1:19–46.
- [13] Brown WE, Chow LC. A new calcium phosphate water setting cement. In: Brown PW, editor. *Cements research progress*. Westerville, OH: American Ceramic Society; 1986. p. 352–79.
- [14] Ginebra MP, Fernandez E, De Maeyer EAP, Verbeeck RMH, Boltong MG, Ginebra J, et al. Setting reaction and hardening of an apatite calcium phosphate cement. *J Dent Res* 1997;76(4):905–12.
- [15] Constantz BR, Barr BM, Ison IC, Fulmer MT, Baker J, McKinney L, et al. Histological, chemical, and crystallographic analysis of four calcium phosphate cements in different rabbit osseous sites. *J Biomed Mater Res (Appl Biomater)* 1998;43:451–61.
- [16] Miyamoto Y, Ishikawa K, Takechi M, Toh T, Yuasa T, Nagayama M, et al. Histological and compositional evaluations of three types of calcium phosphate cements when implanted in subcutaneous tissue immediately after mixing. *J Biomed Mater Res (Appl Biomater)* 1999;48:36–42.
- [17] Chow LC. Calcium phosphate cements: Chemistry, properties, and applications. *Mat Res Symp Proc* 2000;599:27–37.
- [18] Barralet JE, Gaunt T, Wright AJ, Gibson IR, Knowles JC. Effect of porosity reduction by compaction on compressive strength and microstructure of calcium phosphate cement. *J Biomed Mater Res (Appl Biomater)* 2002;63:1–9.
- [19] Yokoyama A, Yamamoto S, Kawasaki T, Kohgo T, Nakasu M. Development of calcium phosphate cement using chitosan and citric acid for bone substitute materials. *Biomaterials* 2002;23:1091–101.
- [20] Ehara A, Ogata K, Imazato S, Ebisu S, Nakano T, Umakoshi Y. Effects of α -TCP and TetCP on MC3T3-E1 proliferation, differentiation and mineralization. *Biomaterials* 2003;24:831–6.
- [21] Apelt D, Theiss F, El-Warrak AO, Zlinszky K, Bettschart-Wolfisberger R, Bohner M, et al. In vivo behavior of three different

- injectable hydraulic calcium phosphate cements. *Biomaterials* 2004;25:1439–51.
- [22] Costantino PD, Friedman CD, Jones K, Chow LC, Sisson GA. Experimental hydroxyapatite cement cranioplasty. *Plast Reconstr Surg* 1992;90:174–91.
- [23] Friedman CD, Costantino PD, Takagi S, Chow LC. BoneSource hydroxyapatite cement: a novel biomaterial for craniofacial skeletal tissue engineering and reconstruction. *J Biomed Mater Res (Appl Biomater)* 1998;43:428–32.
- [24] Ishikawa K. Effects of spherical tetracalcium phosphate on injectability and basic properties of apatitic cement. *Key Eng Mater* 2003;240-242:369–72.
- [25] Khairoun I, Boltong MG, Driessens FCM, Planell JA. Some factors controlling the injectability of calcium phosphate bone cements. *J Mater Sci: Mater in Med* 1998;9:425–8.
- [26] Ginebra MP, Rilliard A, Fernández E, Elvira C, Román JS, Planell JA. Mechanical and rheological improvement of a calcium phosphate cement by the addition of a polymeric drug. *J Biomed Mater Res* 2001;57:113–8.
- [27] Sarda S, Fernández E, Nilsson M, Balcells M, Planell JA. Kinetic study of citric acid influence on calcium phosphate bone cement as water-reducing agent. *J Biomed Mater Res* 2002;61:653–9.
- [28] Ooms EM, Egglezos EA, Wolke JGC, Jansen JA. Soft-tissue response to injectable calcium phosphate cements. *Biomaterials* 2003;24:749–57.
- [29] Gbureck U, Barralet JE, Spatz K, Grover LM, Thull R. Ionic modification of calcium phosphate cement viscosity: Part I: hypodermic injection and strength improvement of apatite cement. *Biomaterials* 2004;25:2187–95.
- [30] Bohner M, Baroud G. Injectability of calcium phosphate pastes. *Biomaterials* 2005;26:1553–63.
- [31] Burguera EF, Xu HHK, Weir MD. Injectable and rapid-setting calcium phosphate bone cement with dicalcium phosphate dihydrate. *J Biomed Mater Res B (Applied Biomater)* (accepted for publication).
- [32] Topoleski LDT, Ducheyne P, Cuckler JM. The fracture toughness of titanium-fiber-reinforced bone cement. *J Biomed Mater Res* 1992;26:1599–617.
- [33] Xu HHK, Quinn JB, Takagi S, Chow LC, Eichmiller FC. Strong and macroporous calcium phosphate cement: Effects of porosity and fiber reinforcement. *J Biomed Mater Res* 2001;57:457–66.
- [34] Burguera EF, Guitián F, Chow LC. A water setting tetracalcium phosphate—dicalcium phosphate dihydrate cement. *J Biomed Mater Res* 2004;71A:275–82.
- [35] Takagi S, Chow LC. Formation of macropores in calcium phosphate cement implants. *J Mater Sci: Mater Med* 2001;12:135–9.
- [36] Cherng A, Takagi S, Chow LC. Effects of hydroxypropyl methylcellulose and other gelling agents on the handling properties of calcium phosphate cement. *J Biomed Mater Res* 1997;35:273–7.
- [37] Xu HHK, Takagi S, Quinn JB, Chow LC. Fast-setting calcium phosphate scaffolds with tailored macropore formation rates for bone regeneration. *J Biomed Mater Res* 2004;68A:725–34.
- [38] Carey LE, Xu HHK, Simon CG, Takagi S, Chow LC. Premixed rapid-setting calcium phosphate composites for bone repair. *Biomaterials* 2005;26:5002–14.
- [39] Xu HHK, Quinn JB. Calcium phosphate cement containing resorbable fibers for short-term reinforcement and macroporosity. *Biomaterials* 2002;23:193–202.
- [40] ASTM Designation D790-03. Standard test methods for flexural properties of unreinforced and reinforced plastics and electrical insulating materials. ASTM: 2003.
- [41] Xu HHK, Quinn JB, Takagi S, Chow LC. Processing and properties of strong and non-rigid calcium phosphate cement. *Journal of Dental Research* 2002;81:219–24.
- [42] Leroux L, Hatim Z, Lacout JL. Effects of various adjuvants (lactic acid, glycerol, and chitosan) on the injectability of a calcium phosphate cement. *Bone* 1999;25:31S–4S.
- [43] Ueyama Y, Ishikawa K, Mano T, Koyama T, Nagatsuka H, Matsumura T, et al. Initial tissue response to anti-washout apatite cement in the rat palatal region: Comparison with conventional apatite cement. *J Biomed Mater Res* 2001;55:652–60.
- [44] Burguera EF, Xu HHK, Takagi S, Chow LC. High early strength calcium phosphate bone cement: effects of dicalcium phosphate dihydrate and absorbable fibers. *J Biomed Mater Res A* (accepted for publication).
- [45] Baroud G, Matsushita C, Samara M, Beckman L, Steffen T. Influence of oscillatory mixing on the injectability of three acrylic and two calcium-phosphate bone cements for vertebroplasty. *J Biomed Mater Res Part B: Appl Biomater* 2004;68B:105–11.
- [46] Simske SJ, Ayers RA, Bateman TA. Porous materials for bone engineering. *Mater Sci Forum* 1997;250:151–82.
- [47] Almirall A, Larrecq G, Delgado JA, Martínez S, Planell JA, Ginebra MP. Fabrication of low temperature macroporous hydroxyapatite scaffolds by foaming and hydrolysis of an α -TCP paste. *Biomaterials* 2004;25:3671–80.
- [48] Bohner M. Calcium phosphate emulsions: Possible applications. *Key Engineering Mater* 2001;192–195:765–8.
- [49] Tsuruga E, Takita H, Itoh H, Wakisaka Y, Kuboki Y. Pore size of porous hydroxyapatite as the cell-substratum controls BMP-induced osteogenesis. *J Biochem* 1997;121:317–24.
- [50] Damien CJ, Parsons JR. Bone graft and bone graft substitutes: A review of current technology and applications. *J Appl Biomater* 1991;2:187–208.
- [51] O'Kelly K, Tancred D, McCormack B, Carr A. A quantitative technique for comparing synthetic porous hydroxyapatite structure and cancellous bone. *J Mater Sci: Mater in Med* 1996;7:207–13.